THE JOURNAL OF BIOLOGICAL CHEMISTRY VOL. 291, NO. 41, pp. 21829–21835, October 7, 2016

Molecular Architecture of Full-length TRF1 Favors Its Interaction with DNA*

Received for publication, June 22, 2016, and in revised form, August 23, 2016 Published, JBC Papers in Press, August 25, 2016, DOI 10.1074/jbc.M116.744896

Jasminka Boskovic[‡1], Jaime Martinez-Gago[§], Marinela Mendez-Pertuz[¶], Alberto Buscato[‡], Jorge Luis Martinez-Torrecuadrada[§], and Maria A. Blasco[¶2]

From the [‡]Structural Biology and Biocomputing Programme, Electron Microscopy Unit, [§]Structural Biology and Biocomputing Programme, Crystallography and Protein Engineering Unit, and [¶]Molecular Oncology Programme, Telomeres and Telomerase Group, Spanish National Cancer Research Centre (CNIO), 28029 Madrid, Spain

Telomeres are specific DNA-protein structures found at both ends of eukaryotic chromosomes that protect the genome from degradation and from being recognized as double-stranded breaks. In vertebrates, telomeres are composed of tandem repeats of the TTAGGG sequence that are bound by a six-subunit complex called shelterin. Molecular mechanisms of telomere functions remain unknown in large part due to lack of structural data on shelterins, shelterin complex, and its interaction with the telomeric DNA repeats. TRF1 is one of the best studied shelterin components; however, the molecular architecture of the full-length protein remains unknown. We have used single-particle electron microscopy to elucidate the structure of TRF1 and its interaction with telomeric DNA sequence. Our results demonstrate that full-length TRF1 presents a molecular architecture that assists its interaction with telometic DNA and at the same time makes TRFH domains accessible to other TRF1 binding partners. Furthermore, our studies suggest hypothetical models on how other proteins as TIN2 and tankyrase contribute to regulate TRF1 function.

Telomeres are the nucleoprotein structures that protect the ends of linear eukaryotic chromosomes from DNA damage-sensing mechanisms and the DNA repair machinery, thus preventing chromosomal fusions and other rearrangements that could lead to genome instability. Telomeres are formed by tandem repeats of the $(TTAGGG)_n$ sequence synthesized by the enzyme telomerase. These repeats are bound by a six-subunit complex called shelterin, which is essential to form the functional telomere. To date, however, the three-dimensional structure of the telomere is unknown, in part due to a lack of structural information on the shelterins and the shelterin complex and its interaction with the telomeric DNA repeats. All shelterin components, except for Rap1, show exclusive binding to TTAGGG repeats and are essential for telomere function and for cell viability, as their deletion in mouse models causes early embryonic lethality (1–5). Rap1, instead, can bind throughout the chromosome arms where it regulates transcription (4, 6). Only two components of the shelterin complex, TRF1[3] and TRF2 (telomeric repeat factors 1 and 2), interact directly with double-stranded telomeric DNA. TRF1 was first to be discovered and is one of the best studied. It was identified as a major protein component of human telomeres (7) that behaves as a negative regulator of telomere length (8, 9). In addition to its known roles in telomere protection and telomere length regulation, TRF1 has been recently proposed to have a role in pluripotency (10) and to be a potential anti cancer target (11). In particular, both genetic and chemical inhibition of TRF1 levels at telomeres has an anti-tumoral effect (11). Two other telomeric proteins, TIN2 and tankyrase, bind to TRF1 and contribute to telomeric length regulation. TIN2 serves as a link between TRF1 and TRF2 and promotes TRF1 interaction with DNA (12). On the other hand, tankyrase promotes the release of TRF1 from the telomeres upon TRF1 PARylation and allows telomere elongation by telomerase (8, 13–15).

The TRF1 protein contains a conserved N-terminal homodimerization domain (TRFH) and a C-terminal DNA binding domain (Dbd) connected by a long loop region (Fig. 1*A*). The N terminus is very acidic and comprises the binding site for tankyrase 1, whereas the TRFH domain is involved in homodimer assembly and in the recruitment of several proteins, including TIN2. The Dbd domain has homology to the single Dbd of Myb oncoproteins, and TRF1 binds to double-stranded telomeric repeats TTAGGG sequence as a preformed dimer. The crystal structures of the TRFH and Dbds domains have allowed a detailed description of the TRF1 domains (16, 17). However, we lack structural information on how the two domains are oriented with respect to each other and how they are organized to form an active TRF1 dimer.

We used the single-particle electron microscopy (EM) technique to obtain first low resolution structures of full-length TRF1 dimer and its structure in complex with telomeric DNA. The protein presents lock-washer-like configuration where the dimerization domains form a scaffold of the protein and the Dbds seem to be in close proximity, facing each other ready to engage telomeric DNA. DNA binding does not introduce big conformational changes on the TRF1 dimer as it interacts with Dbds maintaining the internal part of the TRFH domain accessible to other TRF1 binding partners. This work opens new ave-

* The authors declare that they have no conflicts of interest with the contents of this article.

Codes apoTRF1-EMD-4105 and TRF1 plus DNA-EMD-4106 have been deposited in the EMDataBank.

[1] To whom correspondence may be addressed. Tel.: 34-917-328-000; Fax: 34-912246976; E-mail: jboskovic@cnio.es.

[2] To whom correspondence may be addressed. Tel.: 34-917-328-000; Fax: 34-917328033; E-mail: mblasco@cnio.es.

[3] The abbreviations used are: TRF, telomeric repeat binding factor; SEC, size-exclusion chromatography; SAXS, small angle x-ray scattering; TCEP, Tris(2-carboxyethyl)phosphine; Dbd, DNA binding domain.

nues for a more detailed mechanistic structure-function study on the protection of chromosomal ends and thus of therapeutic strategies targeting telomeres both for cancer and aging.

Results

TRF1 Was Produced as a Dimer Suitable for Structural Analysis—TRF1 protein was expressed in the baculovirus insect cell system and purified to homogeneity. Expression of the recombinant TRF1 resulted in mainly insoluble protein. To increase the solubility of the final protein chaperones Hsp70 and its cofactors, Hsp40 and Hsdj were co-expressed with His-tagged TRF1 (16–19), which undoubtedly improves the solubility of the recombinant protein several-fold. The final product was >95% pure as shown by SDS-PAGE (Fig. 1*B*, *inset*). The molecular weight of the purified protein was assessed by size-exclusion chromatography (SEC), indicating that the TRF1 protein was purified as a dimer (Fig. 1*B*).

TRF1 Domains Are Oriented within a Dimer Ready to Engage dsDNA—To examine the molecular architecture of the TRF1 dimer, we carried out single-particle EM studies. The size (<100 kDa) and shape of the particles are below the limit that can be regularly visualized and resolved at high resolution by cryo-EM. Therefore, we have used the staining agent to increase the signal to noise ratio of the images and to elucidate the three-dimensional structure of TRF1. We first analyzed the structure of the apoTRF1 protein. For that, the freshly purified TRF1 sample was applied directly onto glow-discharged carbon-coated copper grids and negatively stained for EM analysis. A detailed examination of the EM field revealed a relatively homogeneous distribution of particles (Fig. 1*C*). The two-dimensional averages showed particles of similar size but different shape that clearly suggested the presence of a 2-fold symmetry (Fig. 1*D*). These EM images, which represent different views of the protein, indicated a lack of preferential orientation of the sample on the EM grid allowing us to pursue three-dimensional reconstruction of TRF1 protein. An initial three-dimensional model was generated using makeinitialmodel.py algorithm implemented in EMAN2 and refined applying 2-fold symmetry over several rounds of alignment and projection matching until it stabilized. To support the validity of the EM reconstruction we compared two-dimensional class averages, generated without any reference bias, with re-projections of the three-dimensional structure of TRF1, which happened to closely match each other (Fig. 2*A*).

The EM structure of TRF1 at 23 Å resolution revealed a lock-washer-like configuration with a central globular part and two bent arms (Fig. 2*B*). To assign the domains within the three-dimensional structure, available crystal structures were fitted into the density map (Fig. 2*C*). The structural details of the TRF1 were sufficient to unambiguously fit the dimerization domain (1H6O.pdb) that forms a scaffold of the protein (Fig. 2, *C* and *E*). Dbds and the loops that link dimerization and Dbds initially could not be precisely located within the free protein mass. Indeed, the Dbd could be placed either in closer contact with the dimerization domain or at the tip of lock-washer shape molecule (Fig. 2*C*). Nevertheless the crystal structure of two Dbds bound to telomeric dsDNA (1W0T.pdb) fit accurately into the TRF1 apo structure (Fig. 2*D*) undoubtedly allowing

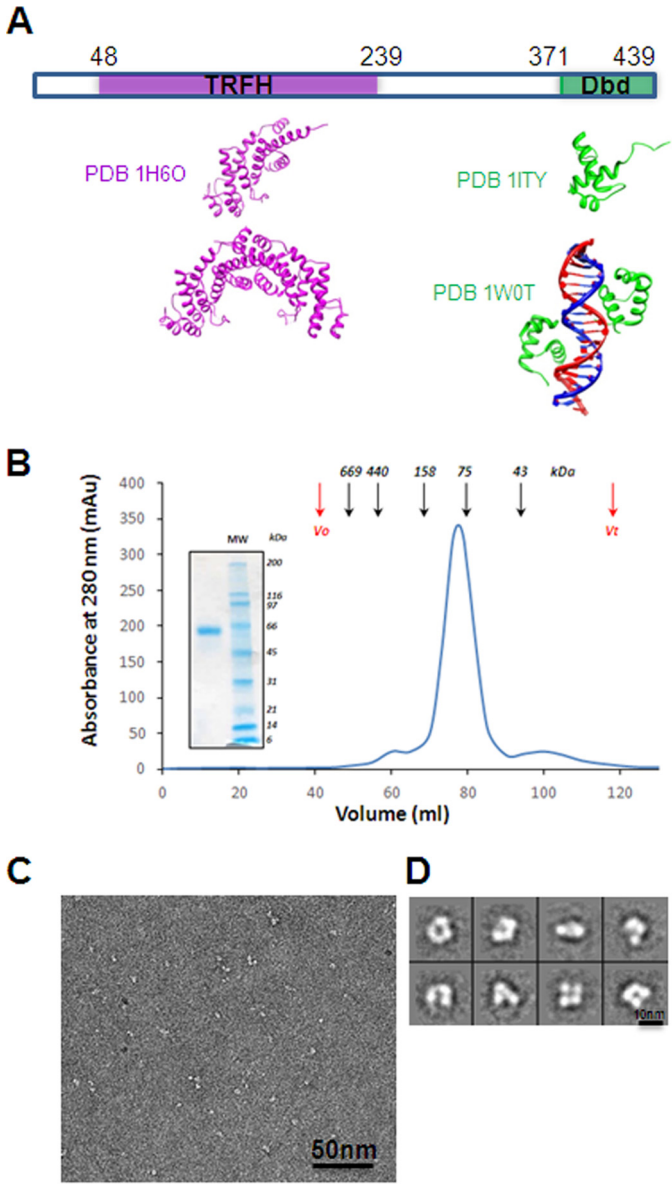

FIGURE 1. **Purification and electron microscopy of TRF1 protein.** *A*, graphic representation of the domain architecture of TRF1 and atomic structures of TRF1 dimerization domain (1H6O.pdb), which forms a dimer, and Dbd (1ITY.pdb) and Dbd in complex with DNA (1W0T.pdb). *B*, elution profile from a SEC of TRF1. The *black arrows* indicate the elution volumes of molecular mass standards (thyroglobulin (669 kDa), ferritin (440 kDa), aldolase (158 kDa), conalbumin (75 kDa), and ovalbumin (43 kDa) and the *red arrows* indicate void volume (*Vo*) blue dextran (2000 kDa) and total volume (*Vt*). The *inset* shows a Coomassie Blue-stained 4–20% SDS-PAGE of purified TRF1 after SEC. *C*, representative field of an electron micrograph obtained for TFR1 after negative staining; *scale bar*, 50 nm. *D*, reference-free two-dimensional averages; *scale bar*, 10 nm.

localization of Dbds (Fig. 2*E*). Thus, in our TRF1 apo structure the Dbds, although connected with the dimerization domain with long and flexible loops, were not randomly oriented but located facing each other with a deflection between them that would allow two Dbds to engage a DNA molecule in opposite sites (Fig. 2*E*).

TRF1 Dimers Bind to Seven TTAGGG Repeats as One Predominant Complex—To examine the interaction of TRF1 with telomeric DNA, we initially performed electrophoretic mobility shift assays (EMSA) with a dsDNA probe containing an array of seven TTAGGG repeats. Gel-shift experiments show that

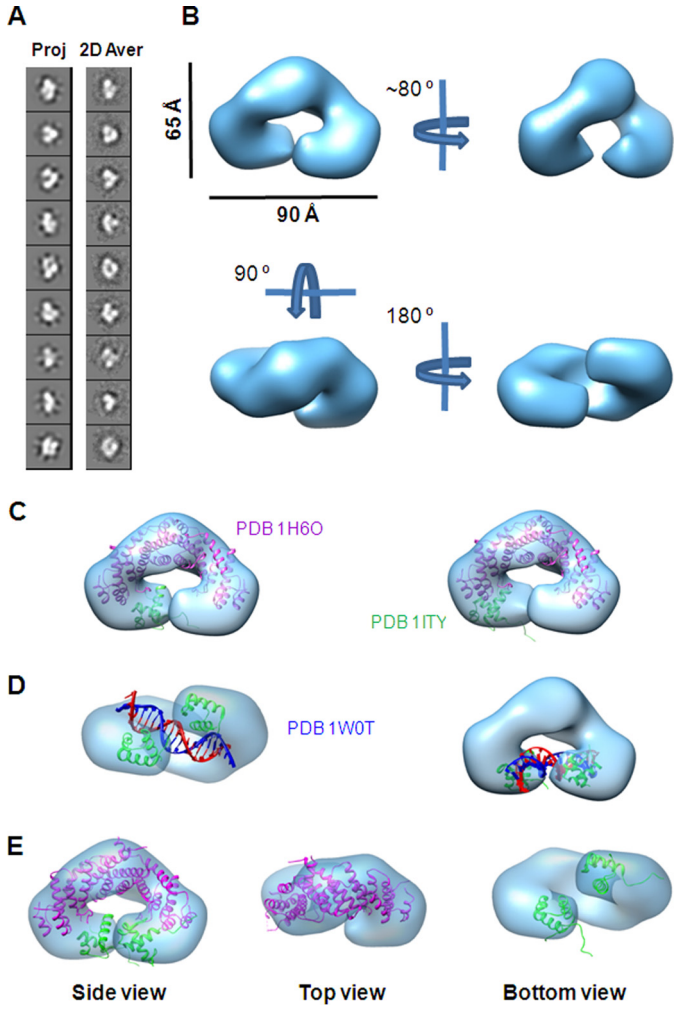

FIGURE 2. **Three-dimensional structure of the TRF1 dimer.** *A*, gallery of selected reference-free two-dimensional averages (*left panel*) compared with the corresponding reprojections of the final structure (*right panel*). *B*, surface representation of the three-dimensional structure of TRF1 obtained after angular refinement. The overall dimensions of the complex are depicted in the figure. *C*, two possible localizations of Dbd (*green*) in apoTRF1 structure. *D*, fitting of atomic structure of Dbds with telomeric DNA (1W0T.pdb) into apoTRF1 structure (*transparent blue*). *E*, several views showing the fitting of the atomic structure of dimerization domain (*1H6O.pdb*) and Dbd domain (*1ITY.pdb*).

TRF1 forms two complexes, one of them clearly predominant (Fig. 3*A*, *lane 2*, lower TRF1 band). To confirm the specificity of these complexes, TRF1 protein was preincubated with specific antibody anti-TRF1 that showed super-shifted TRF1 (Fig. 3*A*, *lane 3*). This effect was not observed with an unspecific antibody (Fig. 3*A*, *lane 4*). Moreover, the addition of excess amounts of unlabeled telomeric probe abolished the formation of TRF1-DNA complex (Fig. 3*A*, *lane 5*).

Binding of Telomeric DNA Does Not Introduce Big Conformational Changes within TRF1 Dimer—To explore putative conformational changes of TRF1 upon its binding to double-stranded telomeric DNA, we prepared and examined the low resolution three-dimensional structure of TRF1-DNA complex and compared it with our apo TRF1 reconstruction. For that we generated a duplex DNA with seven TTAGGG repeats coupled to biotin molecule that included EcoRI restriction site and incubated with purified TRF1 dimer (see "Experimental Procedures"). TRF1-DNA complexes were released from the beads by EcoRI DNA cleavage. The freshly eluted fractions containing the protein-DNA complex were directly applied on carbon-coated glow discharged EM grids and negatively stained for further structural analysis.

Reference-free two-dimensional class averages of DNA-bound complex showed similar general features to apoTRF1 (Fig. 3*B*). Consequently, and to discard any bias during image processing, we used two initial band-passed models: our final apoTRF1 structure and the same starting model used for apo-TRF1. They both converged into the same three-dimensional structure (Fig. 3*C*). The TRF1-DNA three-dimensional reconstruction clearly indicated the presence of extra density between the two Dbds. The presence of the stain excluding region between the two Dbds could be interpreted as a result of the presence of DNA occupying the space between these domains. As was the case with apoTRF1 volume, the crystal structure of TRF1-Dbds bound to telomeric DNA (1W0T.pdb) fitted nicely on the bottom part of the TRF1-DNA volume and further supported the location of the bound telomeric DNA between the tips of the dimeric TRF1 molecule (Fig. 3*D*). Therefore, comparison with the previous EM volume demonstrates that the presence of the DNA did not induce large conformational changes (Fig. 3*E*). Importantly, the orientation between two Dbds domains remained almost the same as in apoTRF1, indicating that the location of the domains in the apo structure was well suited for binding simultaneously to two adjacent and opposite TAGGG binding sites.

Discussion

Telomeres are located at the chromosome ends and are essential for chromosomal stability. This protective function is exerted by binding of the so-called shelterin proteins to telomeric DNA repeats. All of these shelterins except for Rap1 are essential for telomere protection (5, 20), and mutations in some of the shelterin proteins have been found both in premature aging syndromes associated to extremely short telomeres, the so-called telomere syndromes (21, 22), as well as in various familiar and sporadic tumors (23–25). Interestingly TRF1 has also been proposed to have an important role in pluripotent and adult stem cells as well as an anti-cancer target (10, 11). Further advancement in the understanding and therapeutic potential of targeting shelterins in cancer and aging, however, needs a structural knowledge of the shelterins and the shelterin complex and its binding to DNA.

In mammals, shelterin components TRF1 and TRF2 directly bind to double-stranded telomeric repeats and build a platform for recruitment of the rest of the members of shelterin complex, Rap1, TIN2, TPP1, and POT1 proteins. Despite their modest sequence identity, TRF1 and TRF2 have a similar architecture. However, the central part of the dimer interface presents a crucial difference between TRF1 and TRF2 that would prevent heterodimerization (17). For both TRF1 and TRF2, dimerization domain is linked to the DNA binding domain with a long protein loop, suggesting flexible arrangements between protein domains. Indeed, the low resolution small angle x-ray scattering (SAXS) envelope of TRF2 dimer has been recently reported as a highly expended molecule with an elevated degree of flexibility in solution (26). In this conformation two DNA binding

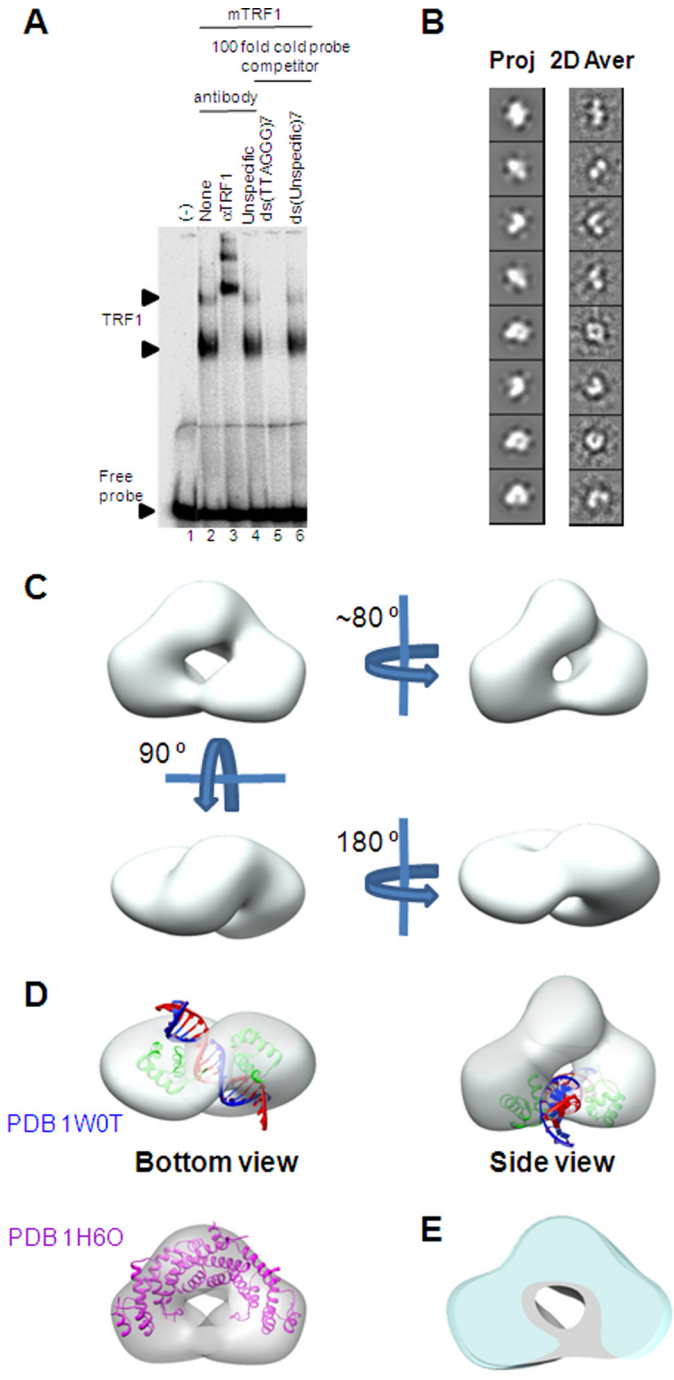

FIGURE 3. **TRF1 DNA binding and three-dimensional reconstruction of TRF1 dimer bound to telomeric DNA.** *A*, TRF1 binding to telomeric dsDNA $(TTAGGG)_7$ *in vitro*. *Arrowheads* show the positions of the two TRF1-containing complexes observed. *Lane 1* did not contain protein; *lane 2*, TRF1: $(TTAGGG)_7$ complexes with no competitor; *lane 3*, with specific antibody against TRF1; *lane 4*, with unspecific antibody; *lane 5*, with 100-fold molar excess of unlabeled probe $ds(TTAGGG)_7$; *lane 6*, with 100-fold molar excess of unlabeled probe $ds(unspecific)_7$ probe. Free probe is indicated. *B*, gallery of selected reference-free two-dimensional averages (*left panel*) compared with the corresponding reprojections of the final structure (*right panel*). *C*, surface representation of the three-dimensional reconstruction of TRF1-DNA complex, obtained after angular refinement, shown in different orientations. *D*, fitting of atomic structures into the TRF1-DNA EM map. The three-dimensional structure of TRF1-DNA is shown as a *white transparent density* with the crystal structures of dimerization domain (*1H6O.pdb*) and Dbd with telomeric DNA (*1W0T.pdb*). *E*, superposition and cut-open views of apo (*light blue*) and DNA-bound (*gray*) structures.

domains are far apart and not facing each other. Yet how TRF1 protein is organized and how it recognizes DNA in the context of the full-length protein is not understood.

To elucidate and analyze the molecular architecture of the full-length TRF1, we have used negative stain single particle electron microscopy. Our three-dimensional EM model of TRF1 revealed a molecule with a lock-washer-like shape where the dimerization domain forms a scaffold of the protein and two Dbds are located relatively close to each other. This difference in protein conformation between the SAXS envelope of TRF2 and the three-dimensional EM structure of TRF1 could be due to the use of two different techniques to address the protein structures; SAXS analysis provides information about the average conformation of the protein in solution, whereas in the case of negative staining EM the protein is attached to the carbon surface of the EM grid. Importantly, the size of the loops that connect the dimerization domain and Dbds is almost 100 amino acids longer in the case of TRF2 dimer compared to the TRF1 loop. This big difference in the length of the unstructured part of the protein could indicate that TRF2 is intrinsically more flexible than the TRF1 dimer, which as a result preferentially could adopt more bent conformation.

In addition, the shape of the dimerization domain of TRF1 provides surfaces for interaction with other proteins (27), like TIN2. TIN2 is a central component of the shelterin complex, which simultaneously binds TRF1 and TRF2, increasing their specificity for telomeres and stabilizing the formation of the protein complex with the telomeric repeat array (28, 29). TRF1 interacts with TIN2 in a way that each TRF1 dimerization domain contacts with one TIN2 molecule (30) (Fig. 4*A*). TIN2 interacts with TRF1 through a stretch of 12 residues forming numerous intermolecular hydrogen-bonding and hydrophobic interactions. Based on the distribution of thermal factors, some of these interactions, particularly in the region of the TIN2 residues 257–262, are quite tight but appear more dynamic near residues Arg-265–Arg-267 (31). The side chain of Arg-266 is nested within a small depression on the TRF1dimerizationsurface, whereas the side chains of residues Arg-265 and Arg-267 are flexible and oriented toward the solvent. We envision that the TIN2 peptide might fill the gap observed between the dimerization domains and the supposedly bound DNA and that the interaction of TIN2 with the DNA through the side chains of Arg-265 and Arg-267 perhaps, consequently, enhance the DNA binding properties of TRF1.

On the other hand, an additional telomeric protein, tankyrase, is essential for TRF1 release from telomeres and facilitates telomere elongation by telomerase. Acidic N-terminal domain of TRF1 is necessary and sufficient for interaction with tankyrase protein through its ANK repeats (32). Hence, tankyrase does not interact with TRF2, as the acidic N-terminal domain is absent from TRF2. The available crystal structure of the ankyrin repeat clusters (ARC2 and ACR3) of tankyrase 1 exhibits a contoured shape that matches to a certain extent the horseshoe shape of the TRF1 dimerization domain (33). The complementarity between the protein surfaces suggests a possible interaction mode between tankyrase and TRF1. Indeed, tankyrase is reported to recognize the N terminus of TRF1 (res-

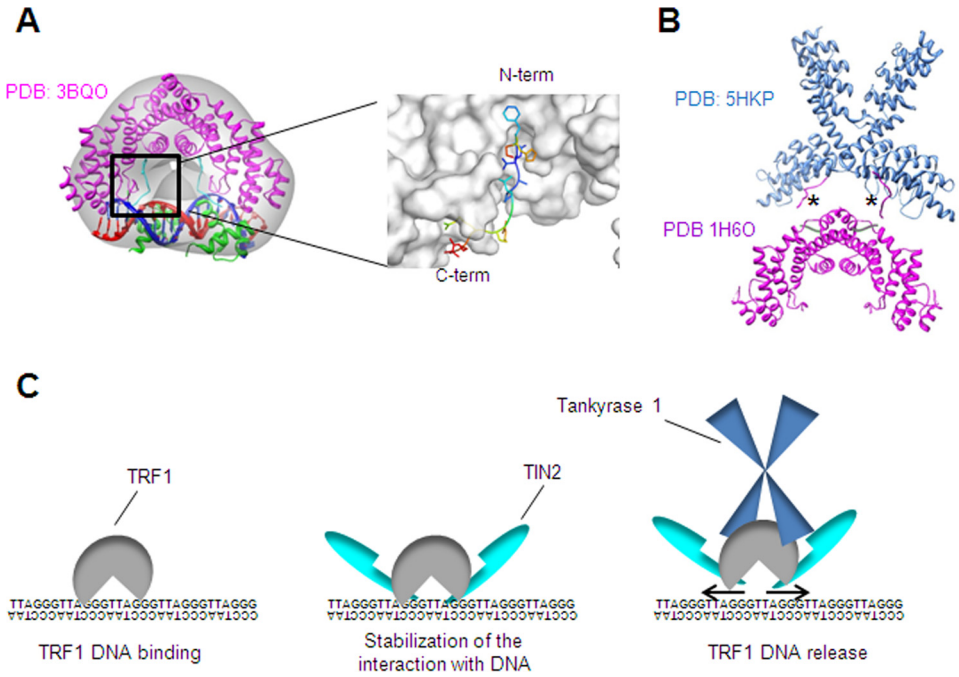

FIGURE 4. **Hypothetical model for TRF1 interaction with telomeric DNA and its release.** *A*, *left*, overall structure of TIN2 peptide (*cyan*) bound to TRF1 dimerization domain (*magenta*) (*3BQO.pdb*). *Right*, a close up of the TRF1 pocket bound to TIN2 peptide. TIN2 peptide is colored by its B-factor showing that C-terminal part of the peptide (*red*) is not in rigid contact with the TRF1 protein (*white transparent surface*). *B*, tankyrase 1 (*5HKP.pdb*) that interacts with N-terminal part of TRF1 (*asterisk*) is modeled with TRF1 dimerization domain to show speculative relative orientation of Tankyrase 1 and TRF1 while forming a complex. *C*, hypothetical model for TRF1 DNA binding and release. TRF1 binds telomeric DNA mainly through its Dbds (*left panel*). The interaction with TIN2 stabilizes the complex with DNA possibly through direct interaction of TIN2 with DNA (*middle panel*). Tankyrase 1 might engage the TRF1 dimer on two opposite sides of the molecule introducing the PARylation and the release of TRF1 (*right panel*).

idues 11–22) located in the outer part of the dimerization domains of TRF1 dimer (Fig. 4*B*). Thus, tankyrase may possibly act as molecular tongs, binding to the TRF1-DNA complex and, in addition to PARylation of TRF1, could transmit conformational changes that separate the TRF1 dimer arms, favoring DNA release and access of telomerase to the telomeric ends (Fig. 4*C*).

In this work we provide a structural basis for understanding how full-length TRF1 interacts with DNA. Our work also suggests potential new insights for TIN2 role in stabilization of TRF1 on DNA and hypothesizes possible TRF1 regulation by tankyrase. Further structural studies will be required to determine the full mechanism of protection of chromosome ends.

Experimental Procedures

Expression and Purification of the Recombinant TRF1 Protein—The mouse full-length TRF1 gene (GenBank™ accession number NM_009352) was amplified by PCR with restriction site-tailed primers incorporating an N-terminal His_6 tag. The resulting DNA was cloned into the BamHI/EcoRI sites of the baculovirus transfer vector pBacPak8 (BD Biosciences; Clontech). The derivative plasmid, pBacPak8-mTRF1, was proof sequenced. Recombinant baculoviruses were obtained from cotransfection of insect Sf9 cells involving Bsu36I-linearized BacPak6 viral DNA (BD Biosciences; Clontech) and the pBacPak8-mTRF1 vector. Positive clones were isolated by plaque assay, and a single recombinant virus, AcTRF1, was purified by a consecutive plaque picking and used to produce a virus stock with a titer of 108 pfu/ml.

For protein expression, Sf9 cells in 500-ml spinner flasks were doubly infected with AcTRF1 virus at a multiplicity of infection of 1.0 and with a dual recombinant baculovirus expressing human chaperone Hsp70 and Hsp40 cofactor (18, 19), kindly provided by Dr. Tsurumi (Aichi Cancer Center Research Institute, Nagoya, Japan), at an multiplicity of infection of 5. After 72 h at 27 °C, infected cells were harvested and resuspended in lysis buffer (20 mM phosphate buffer, pH 7.4, 500 mM NaCl, and 1% Triton X-100) supplemented with a protease inhibitor mixture (Roche Applied Science). After a brief sonication, the lysate was centrifuged (12,000 × *g*, 20 min, 4 °C), and His-mTRF1 in soluble the fraction was purified by affinity chromatography using a HisTrap column (GE Healthcare) on an ÄKTA prime (GE Healthcare). The HisTrap column was washed with buffer A (20 mM phosphate buffer, pH 7.4, 500 mM NaCl, 20 mM imidazole, and 2 mM Tris(2-carboxyethyl) phosphine (TCEP)) and eluted with a stepwise gradient (0–100%) of buffer B (20 mM phosphate buffer, pH 7.4, 500 mM NaCl, 500 mM imidazole, and 2 mM TCEP). TRF1-containing fractions were pooled, concentrated to <5 ml with a 10-kDa Vivaspin concentrator (Sartorius), and further purified by SEC with a Superdex S200 16/600 column (GE Healthcare) in SEC buffer (20 mM Tris, pH 7.5, 30 mM NaCl, and 1 mM TCEP) using an ÄKTA FPLC system (GE Healthcare). Protein standards (GE Healthcare) were loaded onto the column for molecular weight calibration using the same method. Finally, the eluted peak corresponding to TRF1 dimers was collected and concentrated to 0.8 mg/ml with a 10-kDa Vivaspin concentrator. Samples were analyzed by SDS-PAGE, and the identity of TRF1 was confirmed by in-gel tryptic digestion followed by LC-MS/MS analysis.

EMSA—In vitro gel-shift assays were performed essentially as described (34) with an end-labeled double-strand oligonucleotide containing seven tandem TTAGGG repeats. Briefly, DNA probes were prepared by annealing the two oligonucleotides, sense (5′-GGGTTAGGGTTAGGGTTAGGGTTAGGG-TTAGGGTTAGGGTTAGGGCCCCTC-3′) and antisense (5′-GAGGGGCCCTAACCCTAACCCTAACCCTAACCCTA-ACCCTAACCCTAACCC-3′), end-labeled with [γ-^{32}P]ATP (Amersham Biosciences) and T4-polynucleotide kinase (New England BioLabs) and purified by free nucleotide removal spin column (Qiagen). Labeled-DNA probes (0.5 ng) were incubated with 1 μg of purified baculovirus-expressed TRF1 protein for 20 min at room temperature in a 30-μl reaction containing 20 mM HEPES-KOH, pH 7.9, 150 mM KCl, 5% (v/v) glycerol, 4% (w/v) Ficoll, 1 mM EDTA, 0.1 mM $MgCl_2$, 0.5 mM dithiothreitol, and 20 μg of bovine serum albumin, and poly(dI-dC) (1 μg) as the nonspecific competitor (Amersham Biosciences). For supershift analysis, recombinant TRF1 was preincubated with anti-TRF1 antibody (rat homemade) or unspecific antibody (anti-GFP) before EMSA. The DNA-protein complexes were resolved on a 5% non-denaturing polyacrylamide (29:1 acrylamide:bisacrylamide) gel with 0.5× Tris-borate-EDTA, TBE (Sigma) as a running buffer. Gels were dried under a vacuum at 80 °C and autoradiographed.

Assembling the TRF1-DNA Complex—The TRF1 bound to specific biotin-labeled DNA template was purified. To this end, a pair of complementary oligonucleotides was designed containing a biotin (Btn) molecule conjugated at the 5′ end of one oligo, an EcoRI restriction site located 25 base pairs downstream from the biotin, and 7 tandem TTAGGG repeats: 5′-Btn-ACGGTGTATCTACTGTTTGAATTCCCATTAT-CGAAGGCACGTGTATGTATAGAGGGTTAGGGTTAG-GGTTAGGGTTAGGGTTAGGGTTAGGGTTAGGGCC-CCTC-3′ and 5′-GAGGGGCCCTAACCCTAACCCTA-ACCCTAACCCTAACCCTAACCCTAACCCTCTATACAT-ACACGTGCCTTCGATAATGGGAATTCAAACAGTAGA-TACACCGTA. The oligonucleotides were hybridized by mixing them at a final concentration of 50 mM and adding 15 mM sodium chloride to the reaction. The mixture was incubated at 94 °C for 4 min and then cooled down slowly to room temperature. The oligo hybridization was checked in a 2% agarose gel. Initially, the DNA template was bound to streptavidin-covered magnetic beads (Dynabeads M-280 Streptavidin, Thermo Fisher Scientific). For that, 20 μl of streptavidin-covered magnetic beads were washed with water and equilibrated with SEC buffer. Beads were later resuspended in 100 μl of SEC buffer and 3 μl of the hybridized DNA at final concentration of 15 mM. The binding reaction was performed at room temperature for 1 h with constant agitation. Beads were washed with SEC buffer to eliminate the excess of DNA, and 0.1 mg of purified TRF1 was incubated with the beads-DNA for 4 h at 4 °C with gentle agitation. The unbound protein was removed by washing beads three times with SEC buffer. Finally, beads were resuspended in 30 μl of SuRE/Cut Buffer H 1× (Roche Applied Science) together with 10 units of EcoRI (Roche Applied Science) and incubated overnight at 4 °C. Beads were magnetically separated, and the supernatant containing the DNA-TRF1 complex was collected for EM analysis.

EM and Image Processing—For negative staining 4 μl (~0.08 mg/ml) of the each sample was applied onto a freshly glow-discharged carbon-coated 400-mesh copper EM grids (Electron Microscopy Sciences) and incubated for 10 s at room temperature. The grids were sequentially laid on top of two distinct 50-μl drops of MilliQ water, and stripped gently for 2 s, and then laid on the top of two distinct 50-μl drops of a freshly prepared 1% uranyl acetate solution for 1 min, striped gently for 10 s and air dried.

Data were collected on a Tecnai 12 transmission EM (FEI, Netherlands) with lanthanum hexaboride cathode operated at 120 keV. Images were recorded under low-dose conditions with an electron dose of 11–18 $e^-/Å^2$ at 61,320− nominal magnification on a 4k×4k TVIPS TemCam-F416 CMOS camera resulting in a final pixel size at the specimen level of 2.5 Å.

The contrast transfer function (CTF) was determined on micrographs with ctffind3 (35), and its effects were corrected with bctf from bsoft program lsbr.niams.nih.gov). Particle selection was performed semi-automatically with e2boxer.py in EMAN2 (36). A total of 32,880 particles were boxed for apo-TRF1 and 33106 for the DNA-bound TRF1 complex.

Reference-free two-dimensional classification and averaging of the raw datasets were carried out in refine2d.py implemented in EMAN and CL2D from the Xmipp package (37). A large number of class averages were produced with around 20 particles in each class. Two-dimensional averages were visually inspected and used for generating a sub-data set with best particles.

For apoTRF1 structure, we used two-dimensional averages as input into the program e2initialmodel.py implemented in EMAN2 with C2 symmetry to produce eight different initial models. These models were carefully inspected for consistency between original reference-free two-dimensional averages and the models re-projections. The best model was low pass-filtered with a cutoff of 50 Å to minimize model bias and was used as starting model. For TRF1-DNA as a starting model we used the same band-pass-filtered initial model as for the TRF1. In parallel, the band-pass-filtered apoTRF1 volume was used.

Three-dimensional volumes were calculated using an iterative projection-matching approach using libraries from EMAN1.9, EMAN2, and XMIPP. The resolution of structures was estimated at 23 Å for apoTRF1 structure and 25 Å for TRF1-DNA complex using Fourier Shell Correlation, with 0.5 cut-off criterion. The resulting volumes were filtered in Spider to calculate resolution using Butter low pass filtering. The docking of atomic coordinates was performed with UCSF Chimera (38).

Author Contributions—J. M.-G. and J. L. M. T. performed protein expression and purification of the protein and protein-DNA complex. M. M.-P. performed the EMSA studies. A. B. assisted with electron microscopy research. J. B. performed electron microscopy research and contributed to study design. J. B. and M. A. B. wrote the manuscript. M. A. B. designed and directed the study. All authors reviewed the results and approved the final version of the manuscript.

Acknowledgments—The M. A. B laboratory is supported by the Spanish Ministry of Economy and Competitiveness Project SAF2013-45111RETOS and the Fundación Botín. We thank Oscar Llorca and Santiago Ramón for valuable comments and Maria Moreno for critical reading of the manuscript.

References

1. Celli, G. B., and de Lange, T. (2005) DNA processing is not required for ATM-mediated telomere damage response after TRF2 deletion. *Nat. Cell Biol.* **7,** 712–718
2. Hockemeyer, D., Daniels, J. P., Takai, H., and de Lange, T. (2006) Recent expansion of the telomeric complex in rodents: two distinct POT1 proteins protect mouse telomeres. *Cell* **126,** 63–77
3. Karlseder, J., Kachatrian, L., Takai, H., Mercer, K., Hingorani, S., Jacks, T., and de Lange, T. (2003) Targeted deletion reveals an essential function for the telomere length regulator Trf1. *Mol. Cell. Biol.* **23,** 6533–6541
4. Martínez, P., and Blasco, M. A. (2010) Role of shelterin in cancer and aging. *Aging Cell* **9,** 653–666
5. Sfeir, A., Kabir, S., van Overbeek, M., Celli, G. B., and de Lange, T. (2010) Loss of Rap1 induces telomere recombination in the absence of NHEJ or a DNA damage signal. *Science* **327,** 1657–1661
6. Martínez, P., Gómez-López, G., García, F., Mercken, E., Mitchell, S., Flores, J. M., de Cabo, R., and Blasco, M. A. (2013) RAP1 protects from obesity through its extratelomeric role regulating gene expression. *Cell Rep.* **3,** 2059–2074
7. Chong, L., van Steensel, B., Broccoli, D., Erdjument-Bromage, H., Hanish, J., Tempst, P., and de Lange, T. (1995) A human telomeric protein. *Science* **270,** 1663–1667
8. de Lange, T. (2005) Shelterin: the protein complex that shapes and safeguards human telomeres. *Genes Dev.* **19,** 2100–2110
9. Walker, J. R., and Zhu, X. D. (2012) Post-translational modifications of TRF1 and TRF2 and their roles in telomere maintenance. *Mech. Ageing Dev.* **133,** 421–434
10. Schneider, R. P., Garrobo, I., Foronda, M., Palacios, J. A., Marión, R. M., Flores, I., Ortega, S., and Blasco, M. A. (2013) TRF1 is a stem cell marker and is essential for the generation of induced pluripotent stem cells. *Nat. Commun* **4,** 1946
11. García-Beccaria, M., Martínez, P., Méndez-Pertuz, M., Martínez, S., Blanco-Aparicio, C., Cañamero, M., Mulero, F., Ambrogio, C., Flores, J. M., Megias, D., Barbacid, M., Pastor, J., and Blasco, M. A. (2015) Therapeutic inhibition of TRF1 impairs the growth of p53-deficient K-RasG12V-induced lung cancer by induction of telomeric DNA damage. *EMBO Mol. Med.* **7,** 930–949
12. Kim, S. H., Han, S., You, Y. H., Chen, D. J., and Campisi, J. (2003) The human telomere-associated protein TIN2 stimulates interactions between telomeric DNA tracts *in vitro*. *EMBO Rep.* **4,** 685–691
13. De Boeck, G., Forsyth, R. G., Praet, M., and Hogendoorn, P. C. (2009) Telomere-associated proteins: cross-talk between telomere maintenance and telomere-lengthening mechanisms. *J. Pathol.* **217,** 327–344
14. Diotti, R., and Loayza, D. (2011) Shelterin complex and associated factors at human telomeres. *Nucleus* **2,** 119–135
15. Hsiao, S. J., and Smith, S. (2008) function at telomeres, spindle poles, and beyond. *Biochimie* **90,** 83–92
16. Court, R., Chapman, L., Fairall, L., and Rhodes, D. (2005) How the human telomeric proteins TRF1 and TRF2 recognize telomeric DNA: a view from high-resolution crystal structures. *EMBO Rep.* **6,** 39–45
17. Fairall, L., Chapman, L., Moss, H., de Lange, T., and Rhodes, D. (2001) Structure of the TRFH dimerization domain of the human telomeric proteins TRF1 and TRF2. *Mol. Cell* **8,** 351–361
18. Martínez-Torrecuadrada, J. L., Romero, S., Núñez, A., Alfonso, P., Sánchez-Céspedes, M., and Casal, J. I. (2005) An efficient expression system for the production of functionally active human LKB1. *J. Biotechnol.* **115,** 23–34
19. Yokoyama, N., Hirata, M., Ohtsuka, K., Nishiyama, Y., Fujii, K., Fujita, M., Kuzushima, K., Kiyono, T., and Tsurumi, T. (2000) Co-expression of human chaperone Hsp70 and Hsdj or Hsp40 co-factor increases solubility of overexpressed target proteins in insect cells. *Biochim. Biophys. Acta* **1493,** 119–124
20. Martinez, P., Thanasoula, M., Carlos, A. R., Gómez-López, G., Tejera, A. M., Schoeftner, S., Dominguez, O., Pisano, D. G., Tarsounas, M., and Blasco, M. A. (2010) Mammalian Rap1 controls telomere function and gene expression through binding to telomeric and extratelomeric sites. *Nat. Cell Biol.* **12,** 768–780
21. Savage, S. A., Giri, N., Baerlocher, G. M., Orr, N., Lansdorp, P. M., and Alter, B. P. (2008) TINF2, a component of the shelterin telomere protection complex, is mutated in dyskeratosis congenita. *Am. J. Hum. Genet.* **82,** 501–509
22. Walne, A. J., Vulliamy, T., Beswick, R., Kirwan, M., and Dokal, I. (2008) TINF2 mutations result in very short telomeres: analysis of a large cohort of patients with dyskeratosis congenita and related bone marrow failure syndromes. *Blood* **112,** 3594–3600
23. Bainbridge, M. N., Armstrong, G. N., Gramatges, M. M., Bertuch, A. A., Jhangiani, S. N., Doddapaneni, H., Lewis, L., Tombrello, J., Tsavachidis, S., Liu, Y., Jalali, A., Plon, S. E., Lau, C. C., Parsons, D. W., Claus, E. B., *et al.* (2015) Germline mutations in shelterin complex genes are associated with familial glioma. *J. Natl. Cancer Inst.* **107,** 384
24. Calvete, O., Martinez, P., Garcia-Pavia, P., Benitez-Buelga, C., Paumard-Hernández, B., Fernandez, V., Dominguez, F., Salas, C., Romero-Laorden, N., Garcia-Donas, J., Carrillo, J., Perona, R., Triviño, J. C., Andres, R., Cano, J. M., *et al.* (2015) A mutation in the POT1 gene is responsible for cardiac angiosarcoma in TP53-negative Li-Fraumeni-like families. *Nat. Commun* **6,** 8383
25. Ramsay, A. J., Quesada, V., Foronda, M., Conde, L., Martínez-Trillos, A., Villamor, N., Rodríguez, D., Kwarciak, A., Garabaya, C., Gallardo, M., López-Guerra, M., López-Guillermo, A., Puente, X. S., Blasco, M. A., Campo, E., and López-Otín, C. (2013) POT1 mutations cause telomere dysfunction in chronic lymphocytic leukemia. *Nat. Genet.* **45,** 526–530
26. Gaullier, G., Miron, S., Pisano, S., Buisson, R., Le Bihan, Y. V., Tellier-Lebègue, C., Messaoud, W., Roblin, P., Guimarães, B. G., Thai, R., Giraud-Panis, M. J., Gilson, E., and Le Du, M. H. (2016) A higher-order entity formed by the flexible assembly of RAP1 with TRF2. *Nucleic Acids Res.* **44,** 1962–1976
27. Newlon, M. G., Roy, M., Morikis, D., Carr, D. W., Westphal, R., Scott, J. D., and Jennings, P. A. (2001) A novel mechanism of PKA anchoring revealed by solution structures of anchoring complexes. *EMBO J.* **20,** 1651–1662
28. Takai, K. K., Kibe, T., Donigian, J. R., Frescas, D., and de Lange, T. (2011) Telomere protection by TPP1/POT1 requires tethering to TIN2. *Mol. Cell* **44,** 647–659
29. Ye, J. Z., Donigian, J. R., van Overbeek, M., Loayza, D., Luo, Y., Krutchinsky, A. N., Chait, B. T., and de Lange, T. (2004) TIN2 binds TRF1 and TRF2 simultaneously and stabilizes the TRF2 complex on telomeres. *J. Biol. Chem.* **279,** 47264–47271
30. Kim, S. H., Kaminker, P., and Campisi, J. (1999) TIN2, a new regulator of telomere length in human cells. *Nat. Genet.* **23,** 405–412
31. Chen, Y., Yang, Y., van Overbeek, M., Donigian, J. R., Baciu, P., de Lange, T., and Lei, M. (2008) A shared docking motif in TRF1 and TRF2 used for differential recruitment of telomeric proteins. *Science* **319,** 1092–1096
32. Smith, S., Giriat, I., Schmitt, A., and de Lange, T. (1998) Tankyrase, a poly(ADP-ribose) polymerase at human telomeres. *Science* **282,** 1484–1487
33. Li, B., Qiao, R., Wang, Z., Zhou, W., Li, X., Xu, W., and Rao, Z. (2016) Crystal structure of a tankyrase 1-telomere repeat factor 1 complex. *Acta Crystallogr. F. Struct. Biol. Commun* **72,** 320–327
34. Zhong, Z., Shiue, L., Kaplan, S., and de Lange, T. (1992) A mammalian factor that binds telomeric TTAGGG repeats *in vitro*. *Mol. Cell. Biol.* **12,** 4834–4843
35. Mindell, J. A., and Grigorieff, N. (2003) Accurate determination of local defocus and specimen tilt in electron microscopy. *J. Struct. Biol.* **142,** 334–347
36. Tang, G., Peng, L., Baldwin, P. R., Mann, D. S., Jiang, W., Rees, I., and Ludtke, S. J. (2007) EMAN2: an extensible image processing suite for electron microscopy. *J. Struct. Biol.* **157,** 38–46
37. Scheres, S. H., Núñez-Ramírez, R., Sorzano, C. O., Carazo, J. M., and Marabini, R. (2008) Image processing for electron microscopy single-particle analysis using XMIPP. *Nat. Protoc* **3,** 977–990
38. Pettersen, E. F., Goddard, T. D., Huang, C. C., Couch, G. S., Greenblatt, D. M., Meng, E. C., and Ferrin, T. E. (2004) UCSF Chimera: a visualization system for exploratory research and analysis. *J. Comput. Chem.* **25,** 1605–1612